Discover Chemical Engineering

Discover

Research

PID controls: the forgotten bioprocess parameters

Sarah W. Harcum[1] · Kathryn S. Elliott[1] · Bradley A. Skelton[1,2] · Stephanie R. Klaubert[3] · Hussain Dahodwala[4] · Kelvin H. Lee[4,5]

Received: 11 September 2021 / Accepted: 20 January 2022
Published online: 27 January 2022

Abstract

The ambr250 high-throughput bioreactor platform was adopted to provide a highly-controlled environment for a project investigating genome instability in Chinese hamster ovary (CHO) cells, where genome instability leads to lower protein productivity. Development of the baseline (control) and stressed process conditions highlighted the need to control critical process parameters, including the proportional, integral, and derivative (PID) control loops. Process parameters that are often considered scale-independent, include dissolved oxygen (DO) and pH; however, these parameters were observed to be sensitive to PID settings. For many bioreactors, control loops are cascaded such that the manipulated variables are adjusted concurrently. Conversely, for the ambr250 bioreactor system, the control levels are segmented and implemented sequentially. Consequently, each control level must be tuned independently, as the PID settings are independent by control level. For the CHO cell studies, it was observed that initial PID settings did not resulted in a robust process, which was observed as elevated lactate levels; which was caused by the pH being above the setpoint most of the experiment. After several PID tuning iterations, new PID settings were found that could respond appropriately to routine feed and antifoam additions. Furthermore, these new PID settings resulted in more robust cell growth and increased protein productivity. This work highlights the need to describe PID gains and manipulated variable ranges, as profoundly different outcomes can result from the same feeding protocol. Additionally, improved process models are needed to allow process simulations and tuning. Thus, these tuning experiments support the idea that PID settings should be fully described in bioreactor publications to allow for better reproducibility of results.

Abbreviations

CHO	Chinese hamster ovary
CQA	Critical product quality attribute
DB	Deadband
DO	Dissolved oxygen
HT	High-throughput
IgG_1	Immunoglobulin G_1
NCBI	National Center for Biotechnology Information
NIH	National Institutes of Health

Supplementary Information The online version contains supplementary material available at https://doi.org/10.1007/s43938-022-00008-z.

✉ Sarah W. Harcum, harcum@clemson.edu | [1]Department of Bioengineering, Clemson University, 301 Rhodes Engineering Center, Clemson, SC 29634, USA. [2]Present Address: Vaccine Research Center, National Institute of Allergy and Infectious Diseases (NIAID), National Institutes of Health, 9000 Rockville Pike, Bethesda, MD 20892, USA. [3]Department of Chemical and Biomolecular Engineering, Clemson University, Clemson, SC 29634, USA. [4]Department of Chemical and Biomolecular Engineering, University of Delaware, Newark, DE 19713, USA. [5]National Institute for Innovation in Manufacturing Biopharmaceuticals (NIIMBL), University of Delaware, Newark, DE 19713, USA.

PBS Phosphate-buffered saline
PID Proportion-integral–differential
VCD Viable cell density
v/v Volume per volume
VRC Vaccine Research Center
WCB Working cell bank

1 Introduction

Academic and industrial research groups have spent over 30 years developing methods to control Chinese hamster ovary (CHO) cell bioreactors to maximize growth, productivity, and critical product quality attributes (CQAs), while minimizing waste product accumulation [1–5]. High-cell density fed-batch cultures can commonly reach viable cell densities (VCD) of over 40 million cells mL^{-1} [6, 7] and titers over 2 g L^{-1} [8]. Recent process intensification efforts have driven the desire for scale-down models, such as the ambr250 high-throughput (HT) bioreactor system [9, 10]. For most ambr250 studies, the pH, dissolved oxygen (DO), and temperature setpoints are provided by the authors, but rarely are any PID gains or manipulated variable ranges disclosed [11, 12]. Unlike bacterial cultures, setpoint ranges used for CHO cell cultures are relatively narrow, such as setpoints pH 6.9–7.3, temperature setpoints 34–37 °C, and DO setpoints 30–50% [6–11]. Further, there is very little literature on the effects of the PID control gain values and manipulated variables on growth and CQAs for mammalian cell cultures [13].

In the process controls field, there exists a wide range of papers on PID tuning, mainly for traditional chemical processes [14–17]. For biologic processes, most PID tuning studies have focused on microbial fermentation processes [18, 19], where the interaction of pH and DO control is not as strong due to non-bicarbonate buffered systems [20]. Conversely, for mammalian cell cultures, the traditional bicarbonate buffer uses gaseous CO_2 for pH control, which can affect O_2 solubility and thus DO control, and vice versa [21, 22]. Typically to begin PID tuning for a chemical process, the PID gains are set to zero [19]. Other approaches determine response times (lag) and have single process time constants, as the disturbances are assumed to be univariate [15, 16]. These approaches are not practical for a biological process, as (1) high process variations could result in cell death and culture loss if the PID gains were set to zero, and (2) some disturbances may be planned, such as the addition of basic feeds daily. There are also other disturbances which are not pre-planned, such as antifoam additions [23–25]. The alternative approach for tuning PIDs for a biological process is to wait for a known or planned process disturbance and monitor the process response [26]. Using this wait and watch approach has been used by several mammalian cell studies to refine the PID gains and manipulated variable ranges [27, 28]. In Rameez et al., the PID tuning process for an ambr15 bioreactor system for pH control was described. To obtain significantly better pH control, the proportional gain (k_P) was increased eight-fold relative to the default values, and the manipulated variable (CO_2 flow rate) was also increased [29]. As the PID control algorithm affects the entire process, Longsworth et al. tuned PID gains for DO control for a CHO cell culture in a BioFlo 320 bioreactor and monitored DO over the entire culture. After four PID tuning, the DO profile variations were significantly reduced to acceptable levels using the new PID gains [30]. These limited studies indicate that default values provided by the manufacturer of a bioreactor control system are not always optimal. Further, it may be necessary to change both the PID gains and manipulated variable ranges to obtain acceptable process control.

The overall goal of the "CHO genomes to phenomes" project, CHOg2p for short, is to correlate genetic shifts within CHO cells to phenotypic culture outcomes, such as productivity and CQAs. Decreasing productivity is a major sign of genome instability. The ambr250 bioreactor system was selected for this project due to its capabilities to provide a reproducible environment across 12-parallel vessels. The ambr250 bioreactors are scalable vessels representative of common industrial conditions; allowing the effects of genetic variations to be assessed with respect to the phenome. In addition to general culture performance, the multi-vessel configuration allows for the modified cells to be characterized under stresses, such as elevated ammonia, lactate, or osmolarity, in parallel [31–33]. As a well-controlled process was necessary for these genome studies, it was also important that the PID settings were sufficiently robust to provide a consistent and well-controlled environment. It was noted early in these studies that pH and DO control was not acceptable, which resulted in lower culture performance compared to traditional glass vessel systems. Therefore, a series of PID tuning experiments were conducted using one feeding protocol to determine if outcomes could be improved by revised PID settings. This PID tuning work will be described for three experiments, where the third refinement resulted in culture outcomes that were reproducible and comparable to a traditional glass vessel system, where the traditional

glass vessel used a cascade control scheme and the ambr250 used a segmented control scheme. Key contribution of this paper include: (1) An approach to tune PID values when a process model does not exist; and (2) Improved PID values for mammalian cell cultures in the ambr250.

2 Material and methods

2.1 Cell culture

Recombinant CHO-K1 Clone A11 expressing the anti-HIV antibody VRC01 (IgG_1) were donated by the Vaccine Research Center at the National Institutes of Health (NIH). The working cell bank (WCB) of CHO VRC01 cells is within seven to 10 population doubling level (PDL). The WCB cells were stored in 1 mL cryovials, frozen in liquid nitrogen.

2.1.1 Pre-cultures

WCB cells were thawed into 250 mL baffled, vented shake flasks with a 70 mL working volume. ActiPro media (GE Healthcare, now Cytiva) with 6 mM L-glutamine (Sigma-Aldrich) was used. The shake flasks were maintained in an incubator controlled at 5% CO_2 and 37 °C with orbital shaking at 135 rpm. Cells were passaged at least three times in the exponential growth phase (every 2–3 days). The targeted seeding inoculum was 0.4×10^6 cells mL^{-1} and the cultures reached between 3 and 5×10^6 cells mL^{-1} for each passage.

2.1.2 Bioreactors

2.1.2.1 ambr250 bioreactors A 12-way ambr250 HT bioreactor system (Sartorius Stedim, Göttingen, Germany) was used to conduct these experiments. Each vessel had two pitched blade impellers and an open pipe sparger (001-5G25). The bioreactors were inoculated at a target cell density of 0.4×10^6 cells mL^{-1} into ActiPro media; the final working volumes were between 209 and 215 mL. Feeding began on Day 3 at 3% (v/v) for Cell Boost 7a and 0.3% (v/v) for Cell Boost 7b (GE Healthcare, now Cytiva) and continued daily. A pyramid feeding scheme was utilized following the schedule: Boost 7a (v/v)/Boost 7b (v/v); Day 6 to Day 7–4%/0.4%; Day 8 to Day 9–5%/0.5%; Day 10 to Day 11–4%/0.4%; Day 12 to Day 13–3%/0.3%. The ambr250 software tracks the volume of each reactor by accounting for additions, sample volumes and evaporation, such that the actual vessel volume is used to determine the feed volumes. Glucose was also supplemented daily, as needed, starting on Day 3, to maintain the cultures above 4 g L^{-1} until the next feed addition. A premixed 10% antifoam solution was used to control foaming (Cytiva, Q7-2587). The antifoam was delivered at 10 µL increments daily starting between Days 2–4 when needed. Bioreactors were harvested when average viabilities were less than 70%.

Culture temperature was controlled to 36.5 °C. The pH was controlled by sparging carbon dioxide (CO_2) and air, and a base addition via liquid pumps (1 M sodium bicarbonate). For the preliminary and PID tuning experiments, the pH setpoint was 7.0. For the preliminary experiment, the pH setpoint had an initial deadband (DB) of 0.01 units. These setpoints were provided by NIH (cell line originator). For the CHOZN GS23 cell line (in Supplement), the setpoints were also provided by the cell line originator (Millipore Sigma). During the PID tuning experiments, the control PID gains and manipulated variables were adjusted to assess sensitivity. Although the ambr250 has an optional open platform communications (OPC) communication package, it was not used in these studies. There are no literature citations for PID tuning using OPC with the ambr250. The preliminary experiment allowed the base-pump flow rate to vary from 0.1 to 10 mL min^{-1} and the carbon dioxide (CO_2) gas flow rate to vary from 0 to 20 mL min^{-1}. All gases were supplied through the open pipe sparger; a gas overlay was not used. The DO had a setpoint of 50% of air saturation for all ambr250 experiments. A PID control algorithm with four control levels for the DO was used in the preliminary experiments. The initial PID gains and manipulated variable ranges will be described for each experiment and are listed in Tables 1 and 2 for pH and DO, respectively. The number of control levels was varied during the PID tuning process, and the number of control levels will be described.

2.1.2.2 BioStatB bioreactor The traditional glass vessel system used was a water-jacketed 1.0-L vessel controlled via the BioStatB DCU (Sartorius Stedim, Göttingen, Germany, circa 2003). MATLAB (Mathworks) was used to collect data. The MFCS

Table 1 The pH PID gains and manipulated variable ranges

Run	pH setpoint	Manipulated variable (range)		Control parameters				
		Lower: base flow rate (mL min^{-1})	Upper: CO_2 flow rate (mL min^{-1})	Lower DB	Upper DB	k_P	t_I (s)	t_D (s)
Ambr250 defaults	7.0	0–10	0–25	0.03	0.03	10	–[a]	–
Preliminary ambr250: initial values	7.0	0.1–10	0–20	0.01	0.01	10	–	–
First tuning: initial values	7.0	0–10	0–25	0.03	0.01	10	–	–
Second tuning: initial values	7.0	0–1.0	0.1–5.0	–	–	10	100	0.02
Third tuning: initial values	7.0	0–1.0	0.1–5.0	–	–	10	100 Lower 200 Upper	–

The initial pH PID control settings for the progression of ambr250 HT experiments. Also shown are the ambr250 default values for mammalian cell cultures (Version 15.2.1)

[a]Value was 0 or not a used parameter. Control schemes do not allow DBs to be used, if t_I and t_D are non-zero

(multi-fermenter control system) OPC software (Sartorius) was used to communicate between MATLAB and the MFCS data acquisition software (Sartorius). The stir speed was manually adjusted, where the initial stir speed was 150 rpm, and was increased to 200 rpm on Day 6. Gas flow rates (air, O_2 and CO_2) to the bioreactor were controlled using three GFC 17 mass flow controllers (Aalborg, Germany), without any feedback control from DO or pH sensors. DO control was achieved by manually increasing the O_2 enrichment to the gas total stream. CO_2 was maintained at 5% of the total gas flow to aid in pH control. The total gas flow rate was constant, as was the CO_2 flow rate. The MFCS software only controlled temperature and pH via the base addition (pH PID gains, proportional 30%, integral 30 s, and differential 0 s, deadband 0.5%). The off-gas measurements, such as pressure, gas temperature, and oxygen concentration, were collected by a BlueInOne Ferm 1050 (BlueSens, Germany).

The bioreactor was inoculated to a cell density of 0.46×10^6 cells mL^{-1} for a total initial volume of 500 mL. Feeding began on Day 3 at 3% (v/v) for Cell Boost 7a and 0.3% (v/v) for Cell Boost 7b (GE Healthcare, now Cytiva) with daily feed addition. Feeding was conducted according to the following pyramid schedule: Boost 7a (v/v)/Boost 7b (v/v); Day 6 to Day 7–4%/0.4%; Day 8 to Day 9–5%/0.5%; Day 10 to Day 11–4%/0.4%; Day 12 to Day 13–3%/0.3%. Since the BioStatB does not automatically calculate liquid volumes, feed additions were based on the initial vessel volume. Glucose was supplemented daily, as needed, starting on Day 3, to maintain cultures above 4 g L^{-1} until the next feed addition. SE-15 antifoam (Sigma) was used to control foaming. The initial volume of pure antifoam in the bioreactor was 100 µL. For periodic use, the antifoam was diluted in ActiPro at the ratio of 100 µL antifoam into 5 mL ActiPro media. The diluted antifoam solution was delivered in 0.5–1.0 mL increments daily starting after Day 5. The bioreactor was harvested when the cell viability was less than 70%.

2.2 Analytical methods: off-line measurements

Samples were taken daily prior to feed additions to assess glucose and determine if supplemental glucose would be required. Post-feed addition samples were taken to measure glucose and confirm glucose addition calculations. Samples were taken daily prior to feed additions to measure VCD, cell viability, lactate, glutamine, glutamate, ammonia, and titer. VCD and viability were measured using the trypan blue exclusion method with the Vi-Cell XR cell viability analyzer (Beckman Coulter, Brea, CA). Extracellular glucose, lactate, glutamine, glutamate, ammonia, and IgG concentrations were measured using a Cedex Bioanalyzer (Roche Diagnostics, Mannheim, Germany).

3 Results and discussion

Tuning the PID control loops became a priority when it was observed that the titers for the ambr250 cultures were lower than the glass vessel cultures. The glass vessel culture reached a titer of 2.0 g L^{-1} with a peak VCD of 27×10^6 cells mL^{-1}. In comparison, the preliminary ambr250 experiment only reached a titer of 1.3 g L^{-1} with a peak VCD of 39×10^6 cells mL^{-1}. This was surprising, since the glass vessel controller required manual gas flow control adjustments, i.e., there was no feedback loop between the gas flow rates and the DO and pH control. The DO was allowed to remain higher than the

Table 2 DO PID gains and manipulated variables by control level

Run	Level	Manipulated variable	Range	Control parameters		
				K_P	K_I	K_D
ambr250 defaults (Version 15.2.1)	0	Stir	400 rpm	–	–	–
	1	Gas	0.05–0.05 mL min^{-1}	10	–	–
	2	Headspace	20–20 mL min^{-1}	10	–	–
	3	O_2 Add	0–10 mL min^{-1}	0.015	500	–
Preliminary ambr250 Initial values	0	Stir	300 rpm	–	–	–
	1	Gas	2–25 mL min^{-1}	0.1	500	–
	2	O_2 Mix	0–100%	0.1	500	–
	3	O_2 Add	0–25 mL min^{-1}	0.015	500	–
	4	Stir	300–600 rpm	3.5	250	–
First tuning Initial values	0	Stir	300 rpm	–	–	–
	1	Gas	2–10 mL min^{-1}	0.1	500	–
	2	Stir	300–400 rpm	0.1	500	–
	3	Gas	10–15 mL min^{-1}	0.015	500	–
	4	O_2 Mix	0–25%	0.015	500	–
	5	Stir	400–450 rpm	0.1	500	–
	6	Gas	15–20 mL min^{-1}	0.1	500	–
	7	O_2 Mix	25–50%	0.015	500	–
	8	Stir	450–500 rpm	0.1	500	–
	9	Gas	20–25 mL min^{-1}	0.1	500	–
	10	O_2 Mix	50–75%	0.015	500	–
	11	Stir	500–600 rpm	0.1	500	–
	12	O_2 Mix	75–100%	0.015	500	–
	13	Stir	600–750 rpm	0.1	500	–
	14	O_2 Add	0–10 mL min^{-1}	0.015	500	–
First tuning Revised values	0	Stir	300 rpm	–	–	–
	1	Gas	2–10 mL min^{-1}	0.1	250	–
	2	Stir	300–400 rpm	0.1	250	–
	3	Air	10–15 mL min^{-1}	0.1	250	–
	4	O_2 Mix	0–50%	0.015	250	–
	5	Stir	400–500 rpm	3.5	250	–
	6	Gas	15–20 mL min^{-1}	0.1	250	–
	7	Stir	500–600 rpm	3.5	250	–
	8	O_2 Mix	50–80%	0.015	250	–
	9	O_2 Add	0–10 mL min^{-1}	0.015	250	–
	10	Stir	600–700 rpm	3.5	250	–
Second tuning Initial values	0	Stir	300 rpm	–	–	–
	1	Gas	2–20 mL min^{-1}	0.1	100	–
	2	O_2 Mix	0–50%	0.05	100	0.02
	3	Stir	300–400 rpm	2	100	–
	4	O_2 Mix	50–100%	0.05	100	0.02
	5	Stir	400–600 rpm	1	100	–
	6	O_2 Add	0–10 mL min^{-1}	0.1	100	–
Third tuning Initial values	0	Stir	300 rpm	–	–	–
	1	Gas	2–20 mL min^{-1}	0.1	100	–
	2	O_2 Mix	0–50%	0.15	100	0.02
	3	Stir	300–400 rpm	2	100	–
	4	O_2 Mix	50–100%	0.15	250	0.02
	5	Stir	400–850 rpm	1.0	100	–
	6	O_2 Add	0–10 mL min^{-1}	0.5	100	–

Table 2 (continued) Initial PID pH control settings for the preliminary and PID tuning experiments. Additionally, ambr250 default values for mammalian cell cultures are shown for version 15.2.1 of the control software

setpoints for most of the glass vessel experiment to compensate for the lack of feedback control. The VCD and metabolites for both the glass vessel and preliminary ambr250 bioreactors are shown in Fig. 1. The three on-line parameters (pH, DO, and stir speed) are shown for comparison between the glass vessel and preliminary ambr250 bioreactors. The most significant difference is the pH profile, where the ambr250 profiles go significantly above the setpoint of pH 7.0 (setpoint shown as green line). The consequence of an elevated pH profile directly correlates with the elevated lactate concentrations, which exceeded 2.0 g L^{-1} (Fig. 1B). It is well-known that lactate consumption occurs more efficient under lower pH levels, due to the lactate transport protein (H + -linked monocarboxylate transporters) being a dual H + /lactate carrier protein [34]. Interestingly, the VCDs (Fig. 1A) were acceptable for the ambr250 experiment, and characteristic lactate consumption was observed; however, the cell specific productivity was significantly lower for the ambr250 cultures compared to the glass vessel cultures.

Often when PIDs are to be tuned, a simulation of the process will be used [17]. This approach has been successful for *Escherichia coli* fermentations and similar fermentations [19, 35, 36]; however, when the media is buffered with bicarbonate, and CO_2 gas is used to control pH, the interactions between CO_2 and oxygen sparging become complex [37]. For example, cells secrete acid and lactate, which can decrease the pH. Later in the culture, lactate can be consumed by the cells, which would increase the pH and decrease osmolarity [38]. High osmolarity feeds are often used, such as the ActiPro feeds. Both pH and osmolarity variations change the saturation equilibrium for both CO_2 and oxygen [39, 40]. Some researchers have attempted to describe these interaction effects, however, not intending to be used in process control algorithm [21, 22, 41, 42]. There is currently no process model that accurately represents these multiple interaction effects for mammalian cell cultures that can be integrated into process control simulation [43], as are available for bacteria and yeast fermentations [44]. Thus, trial and error PID tuning is one approach to improve the PID settings for ambr250 bioreactors.

Throughout the preliminary ambr250 experiment, several interventions were attempted to bring the pH back to the setpoint. These interventions were limited to adjusting the manipulated variables. First, the lower pH loop setpoint was reduced to pH 6.9 on Day 6, and the upper pH loop setpoint was reduced to pH 6.9 on Day 7 (Fig. 2A). Second, the sparge gas flow rates and stir speed were adjusted with the intent to improve the DO response; however, these adjustments affected the pH profiles as well, known as interaction effects. Specifically, on Day 6.5, the maximum O_2 added flow rate was increased from 25 to 45 mL min^{-1} and the maximum stir speed was increased from 600 to 700 rpm. These adjustments restored DO to the setpoint, but also increased the pH (Fig. 2B). Next, the maximum O_2 added flow rate was decreased from 45 to 20 mL min^{-1} and the stir speed maximum was changed from 700 to 900 rpm. Finally, on Days 7 and 7.2, the maximum O_2 added flow rate was decreased from 20 to 10 mL min^{-1}, and then increased from 10 to 25 mL min^{-1}, respectively. The maximum O_2 added flow rate modifications had minor effects on pH and the increased maximum stir speed stabilized the DO control, yet, stir speeds above 600 rpm were not recommended by the NIH VRC researchers who donated the cell line (Joe Horwitz, personnel communication). Additionally, the pH control was still an issue. As a robust bioreactor environment was desired, PID tuning was undertaken to improve both pH and DO control without resorting to stir speeds above 600 rpm.

It is common in bioprocessing to solely use PID control algorithms versus model based control due to robust behavior and simplicity of PID control [25, 28]. The ambr250 HT system has several process parameters that can be controlled to setpoints by PID control algorithms, such as temperature, pH, and DO. The antifoam addition also can be controlled by a PID algorithm that utilizes bioreactor pressure and the foam level sensor. Confounding pH and DO controls are the interdependencies of these process parameters on each other, yet the PID responds independently. For example, the DO control algorithm uses no knowledge of the pH yet pH shifts due to base or feed additions can cause sudden degassing of the culture due changes in Henry's constant. Simple PID controllers do not use this information. In the preliminary ambr250 experiment, it was observed that manipulated variables inadvertently impacted other process parameters. For example, when the stir speed was allowed to change faster to control the DO, it had a more pronounced effect on the pH (Fig. 2C, D, Day 7.7). Further, tuning the PID gains for pH can impact DO response and vice-versa.

There are two basic formalisms for PID controls used in bioreactor control units. For the ambr250 the PID controller, the "Output" is determined by the "Deviation" or difference from the setpoint (also called the error) using the following equation:

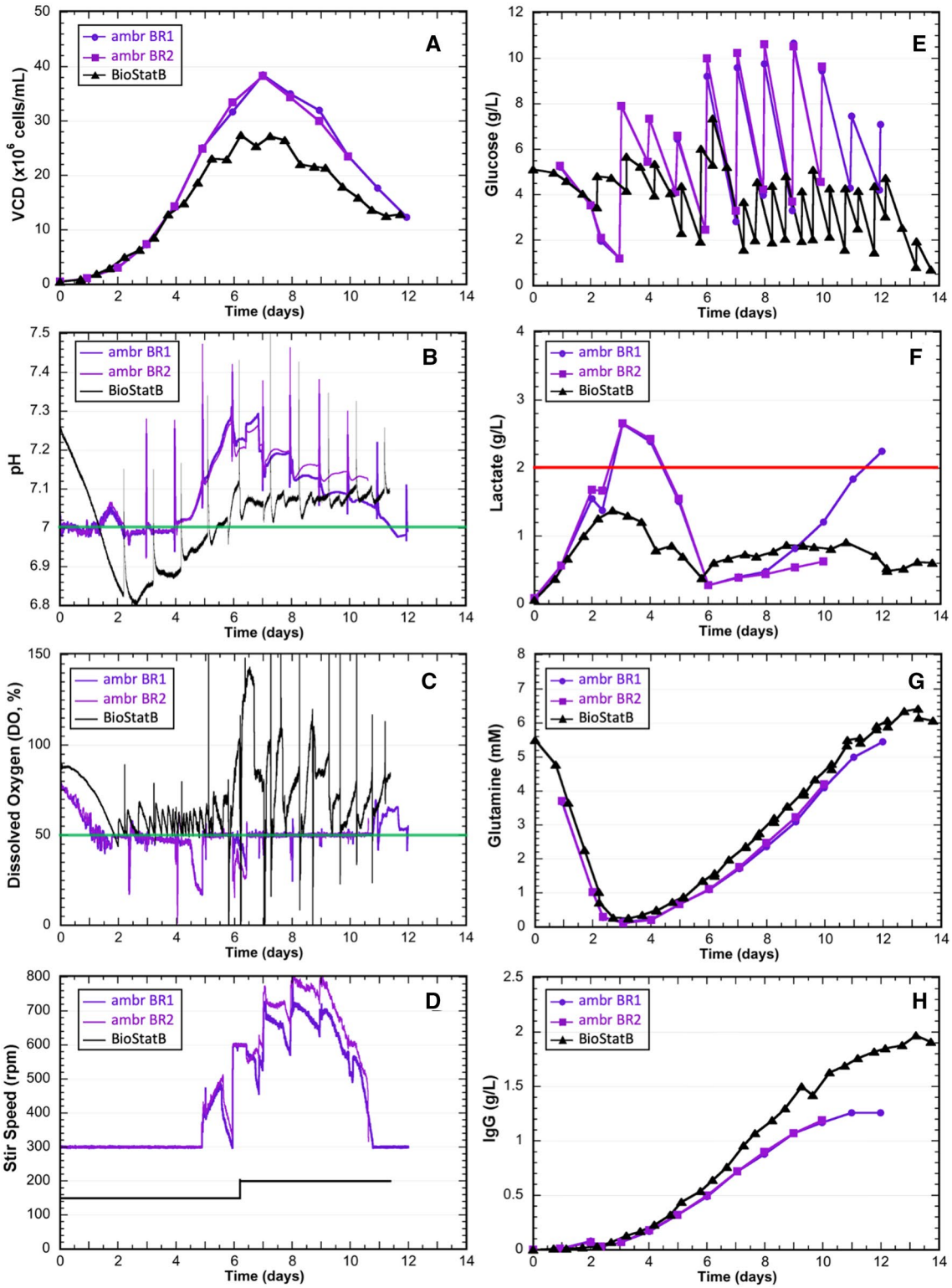

Fig. 1 Growth, pH, DO, stir speed and metabolite profiles. CHO VRC01 cells were cultured in the ambr250 in duplicate and compared to BiostatB bioreactor cultures. **A** Viable cell density (VCD). **B** pH. **C** DO. **D** Stir speed. **E** Glucose. **F** Lactate. **G** Glutamine. **H** IgG (titer). The preliminary ambr250 bioreactors are shown as two shades of purple, while the BiostatB data is shown in black. The green horizontal lines in **B** and **C** indicate the pH and DO setpoints, respectively. The red horizontal line in **F** indicates the maximum lactate concentration to ensure no growth inhibition [45]

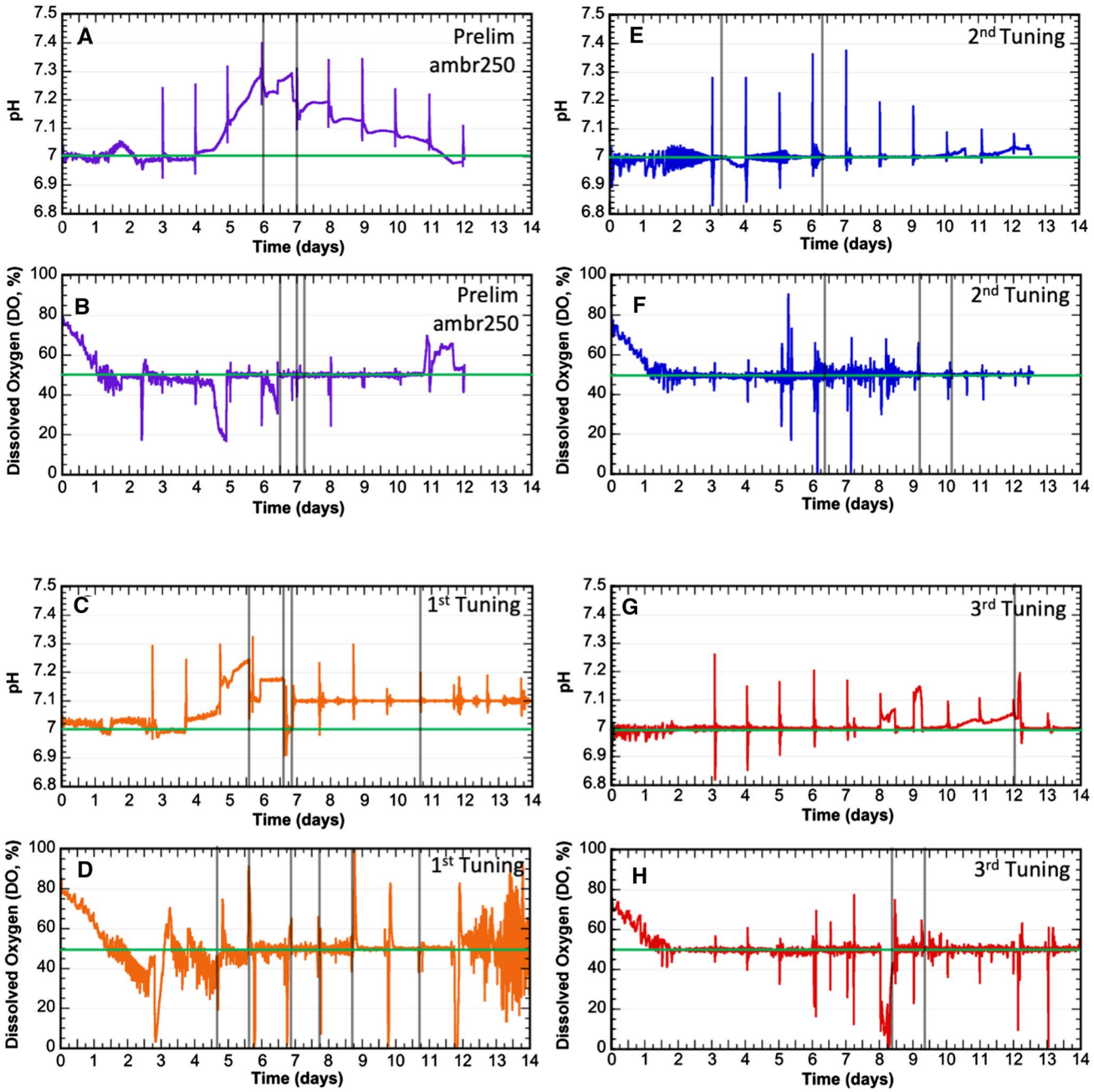

Fig. 2 PID tuning pH and DO profiles. CHO VRC01 were cultured in the ambr250, where the PID gains and manipulated variable ranges were evaluated with respect to pH and DO stability. The pH profiles are shown in panels **A**, **C**, **E** and **G**. The DO profiles are shown in panels **B**, **D**, **F**, and **H**. **A** and **B** Preliminary ambr250 experiment (purple). **C** and **D** First PID tuning experiment (orange). **E** and **F** Second PID tuning experiment (blue). **G** and **H** Third PID tuning experiment (red). The vertical lines in grey indicate when PID gains or manipulated variable ranges were changed from the initial values. The green horizontal lines in **A**, **C**, **E** and **G** indicate the pH setpoints. The green horizontal lines in **B**, **D**, **F** and **H** indicate the DO setpoints

$$Output = k_P\left(Deviation + \frac{1}{t_I}\int Deviation\,dt + t_D\frac{d(Deviation)}{dt}\right).$$

where, k_P is the proportional constant (unitless); t_I is the integral constant (s); and t_D is the derivative constant (s). The k_P, t_I, and t_D constants are call the PID gains [28]. Notice that the k_P term is multiplied across all three equation components in this formalism. Conversely, for the BiostatB controller, the k_P term only multiples the first term. The output values determine the magnitude of the response by the manipulated variable, such as the stir speed. Thus, the output value

would be different for the same PID gains and deviation, depending on the formalism. As the effect of the k_P term on the output is affected by the equation structure, it is important to know the formalism of a particular controller.

In addition to the PID gains and manipulated variable ranges, bioreactor controllers can have the capability to simultaneously or sequentially implement PID gains. The ambr250 bioreactor PID gains are sequentially used by control level. Figure 3 graphically depicts the manipulated variables by control level for DO for the preliminary and PID tuning experiments. Table 2 lists the initial PID gains and manipulated variable ranges for DO control for the preliminary and the three PID tuning experiments. As it is not practical to set the PID gains to zero for a bioreactor, the preliminary ambr250 experiment observations and a series of PID tuning experiments were used to observe output responses to planned disturbances to improve the pH and DO control in the ambr250 for CHO cell lines.

3.1 First pH PID tuning experiment

As the pH control algorithm is simpler with a single control level, all the pH PID tuning experiments will be discussed prior to the DO PID tuning experiments. The three PID tuning experiments investigated both pH and DO simultaneously, and interaction effects will be noted. For pH control, the PID gains used in the preliminary experiment were similar to the default ambr250 default PID gain values, though the preliminary experiment used slightly tighter DBs, per the recommendations of the VRC01 cell line donor. Table 1 lists the pH PID gains and manipulated variable ranges for the ambr250 default values, the preliminary experiment, and the initial values for each PID tuning experiment. For the BioStatB glass vessel, pH control was achieved by utilizing a constant CO_2 flow rate and PID gain controlled base additions to increase the pH. If the pH was too high, the CO_2 flow rate had to be manually adjusted. In contrast, for the ambr250, pH control was divided into upper and lower control limits, each of which could be varied independently. The preliminary ambr250 setpoint was pH 7.0 for both lower and upper limits. The manipulated variable ranges were different due to strength of the fluid used (Table 1), such as sodium bicarbonate for the lower limit and CO_2 flow rate for the upper limit.

If the DB is too narrow, one could observe alternating base additions and CO_2 flow, which would result in increased culture osmolarity. Thus, to prevent this potential oscillatory behavior, the pH PID gains were increased from 0.01 to 0.03 for the upper DB, and the manipulated variable, maximum CO_2 flow rate, was increased from 20 to 25 mL min^{-1}. The proportional gain (k_P) was unchanged from 10 (unitless). On Day 5.6, the pH was observed to be increasing, and had reached pH 7.2. To gauge the sensitivity of the pH control, the upper limit DB was decreased from 0.03 to 0.01 (Fig. 2C). This immediately decreased the pH to ~ 7.1, where it remained stable. Interestingly, an addition of antifoam on Day 5.8 resulted in the pH reaching a slightly higher, yet stable value of pH 7.18. On Day 6.6, the pH was still unacceptablly high, the k_P term was increased from 10 to 12 (unitless). This increase quickly caused the pH to decrease to ~ 6.95 (Fig. 2C); however, feed and antifoam additions occurred immediately after this adjustment, which increased the stable pH to 7.1. In order to prevent pH overshoots, on Day 6.8, the maximum base addition flow rate was decreased from 10 to 1.0 mL min^{-1}. Additionally, the DB was removed on both the upper and lower limits and replaced by k_P 10, t_I 100 s and t_D 0.02 s, as both DB and t_I/t_D cannot be used simultaneously. This change coincided with the peak VCD and the culture was already in the lactate consumption phase (Fig. 4A, B). The next four feed additions were reflected in spikes in the pH profile. Though the pH was still above the setpoint, it generally remained stable (Fig. 2C). To determine the effect of the CO_2 flow rate, the maximum CO_2 flow rate was decreased from 25 to 8 mL min^{-1} and the t_D was set to 0.05 s on Day 10.7. As expected, the next three feed additions resulted in pH spikes with some oscillatory behavior, but in general the pH control was stable. However, the pH was still significantly above the setpoint at pH 7.1 (Fig. 2C). Thus, a second tuning experiment was required to address the elevated pH.

3.2 Second pH PID tuning experiment

To address the stable, but elevated pH, the second tuning experiment initially used a k_P base addition flow rate (lower limit) that matched those at the end of the first tuning experiment (0 to 1.0 mL min^{-1}), while the maximum CO_2 flow rate (upper limit) was decreased from 8.0 to 5.0 mL min^{-1}. Table 1 lists the initial PID gains and the manipulated variable ranges. The PID gains for both limits were set to k_P 10, t_I 100 s and t_D 0.02 s, which resulted in stable pH control in the first tuning experiment. In this second tuning experiment, the pH profile during the first two days of culture oscillated more than in the previous experiment, but remained between pH 6.95 and 7.05 (Fig. 2E). When the first feed addition occurred on Day 3, the pH spiked up to pH 7.25, then fell to nearly pH 6.8. This overshooting behavior was more than desired, so on Day 3.3, the t_D term was decreased from 0.02 to 0.01 s. Interestingly, the pH decreased slightly. On Day 4, the t_D term was further decreased from 0.01 to 0 s. The feed addition on Day 4.1 resulted in another pH spike up to

Fig. 3 Manipulated variable ranges, gas flow rates and stir speed across the PID tuning experiments. Multiple control levels were used by the ambr250 bioreactors for DO control. The manipulated variables are: total gas flow rate to the sparge gas (Gas flow rate, green), O_2 enrichment into the air/gas stream (O_2 mix, blue), added O_2 flow rate to the gas flow rate (O_2 added flow, purple), and the stir speed (Stir speed, red). The total gas flow rate is the sum of the air and O_2 flow rates, where initially the gas is 100% air. The O_2 mixture percentage increases to control DO until the gas flow rate is 100% O_2. Panels **A**–**D**, respectively, show the graphical representations of the manipulated variables for the preliminary ambr250 and the successive PID tuning experiments. Panels **E**–**H**, respectively, show the actual air flow rate (green), O_2 flow rate (blue), and stir speed (red) for the preliminary ambr250 experiment and the successive tuning experiments

pH 7.25; however, the downward spike was only to pH 6.85 (a slight improvement), before stabilizing to a pH of pH 7.0. When feeds were added on Days 5 and 6, upward spike behavior remained consistent, yet the downward spikes were smaller; however, the pH would oscillate briefly after each feed addition. Per Ziegler, dampening oscillations with a stable response is considered a stable control strategy [15]. Thus, on Day 6.3, the t_I term was increased from 100 to 200 s. This change resulted in shorter pH oscillation post-feed addition (Fig. 2E).

3.3 Third pH PID tuning experiment

During the second PID tuning experiment, there was no opportunity to test the pH lower limit of the PID gains. Accordingly, the third pH PID tuning experiment used the same initial k_P and t_I terms from the second experiment. Similar to the second PID tuning experiment, the pH initially oscillated; however the amplitudes were smaller for the third PID tuning experiment. When the first feed addition occurred on Day 3, the pH responses are indistinguishable between the second and third PID tuning experiments (Fig. 2E, G). Conversely, the feed additions on Days 4.5 through Day 7.5 resulted in lower magnitude changes compared to the second experiment. Interestingly, the observed elevated pH on Day 9, can be attributed to the DO PID tuning that started on Day 8.4 (Fig. 2H). Then, beginning on Day 10, the pH began to increase slowly above the setpoint, such that by Day 12, this deviation was greater than desired. To address this deviation, the maximum CO_2 flow rate was increased from 5 to 8 mL min^{-1}. This adjustment decreased the pH back to the setpoint. By comparing the pH profiles from the preliminary experiment (Fig. 2A) to the third tuning experiment (Fig. 2G), a clear improvement in the pH control was achieved. For future experiments, the upper limit PID gains will be k_P 10, t_I 100 s and t_D 0.0 s, with the CO_2 flow rate range of 0.2 to 8 mL min^{-1}. The improved pH control can also be linked to reduced lactate accumulation throughout the cultures (Fig. 3B).

3.4 DO PID tuning experiments

DO control is more complex than pH control in bioreactors, as there are often more manipulated variables (total gas flow rate, O_2 enrichment of the sparge gas, stir speed and option to sparge the headspace). Furthermore, the ambr250 has the added complexity of multiple control levels, where the PID gains and manipulated variable ranges can each be varied independently by control level. To illustrate this complexity, the preliminary manipulated variable ranges are shown graphically in Fig. 3A. In control level 1, the stir speed is set to 300 rpm and the total sparge gas flow rate can be varied from 2 to 25 mL min^{-1}. The O_2 enrichment of the total gas sparge stream is 0%, i.e., the sparge gas is all air. When DO control is no longer achieved by a 300 rpm stir speed and 25 mL min^{-1} air sparging, the controller moves up to control level 2. In control level 2, the sparge gas can be enriched with up to 100% O_2. When DO control is no longer achieved with 300 rpm stir speed and 25 mL min^{-1} 100% O_2 gas sparging, the controller moves up to control level 3. In control level 3, the 100% O_2 gas sparged flow rate can increase from 25 to 50 mL min^{-1}, while the stir speed remains at 300 rpm. When DO control is no longer achieved with 300 rpm stir speed and 50 mL min^{-1} 100% O_2 gas sparging, the controller moves up to the final control level (control level 4). In control level 4, the stir speed can increase from 300 to 600 rpm, while 50 mL min^{-1} 100% O_2 gas sparging continues (Fig. 3A). Figure 3B–D show the manipulated variable ranges for the DO PID tuning experiments. The PID gains used for the preliminary experiment are listed for all the tuning experiments in Table 2 by control level and the PID gains for each control level. Further, the stir speeds, air, and O_2 flow rates for the preliminary ambr250 experiment are shown in Fig. 3E for comparison. Figure 3F–H show the stir speeds, air, and O_2 flow rates for the DO PID tuning experiments. The experimental stir speeds excessed these initial stir speeds due to adjustments to the manipulated ranges and these adjustments will be discussed later. For the DO control in the preliminary experiment, only manipulated variables were changed in an attempt to better control the DO to the setpoint of 50% saturation (shown as a green line in Fig. 2B, D, F, H).

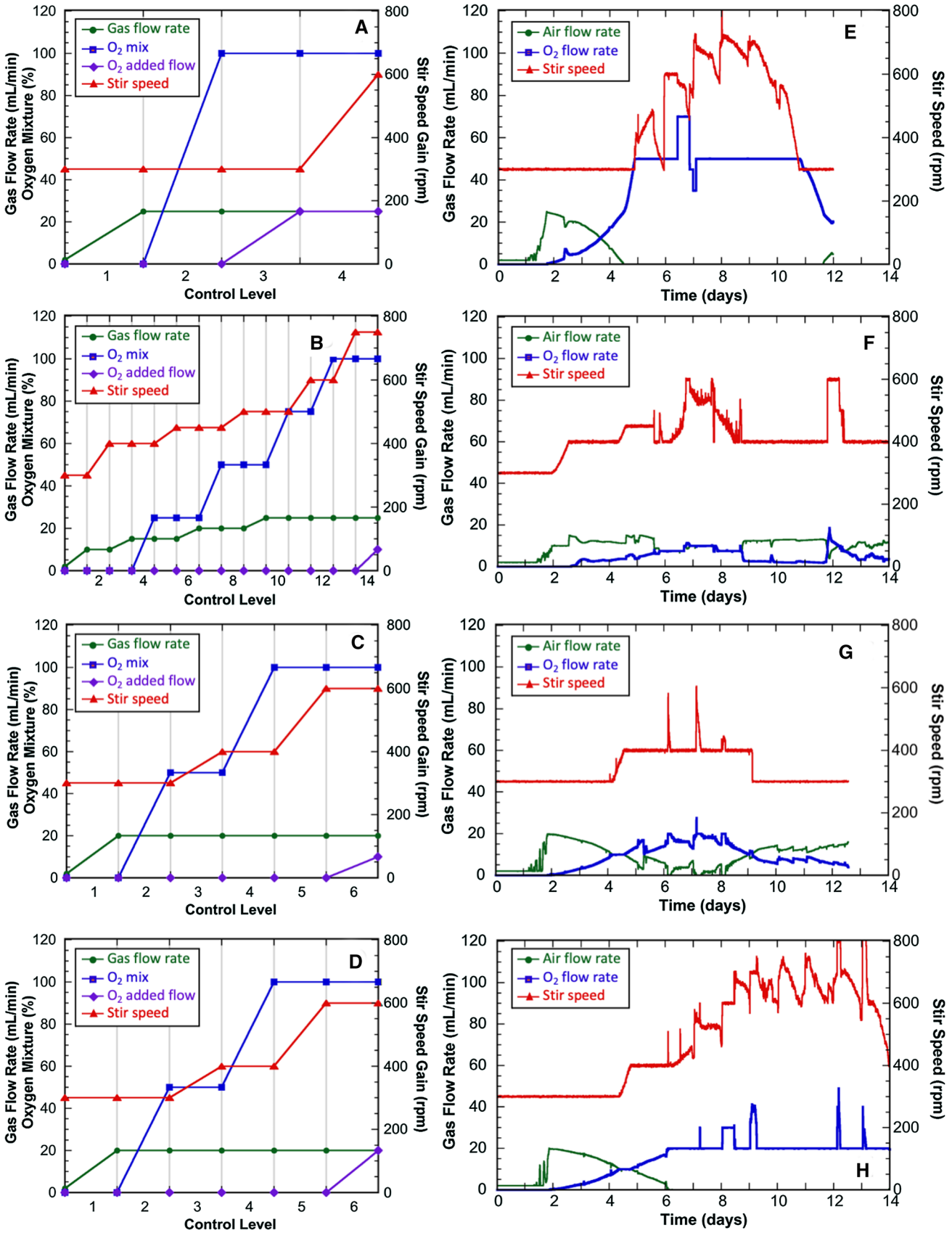
A
Gas flow rate
O_2 mix
O_2 added flow
Stir speed
Gas Flow Rate (mL/min)
Oxygen Mixture (%)
Stir Speed Gain (rpm)
Control Level
B
C
D
E
Air flow rate
O_2 flow rate
Stir speed
Gas Flow Rate (mL/min)
Stir Speed (rpm)
Time (days)
F
G
H

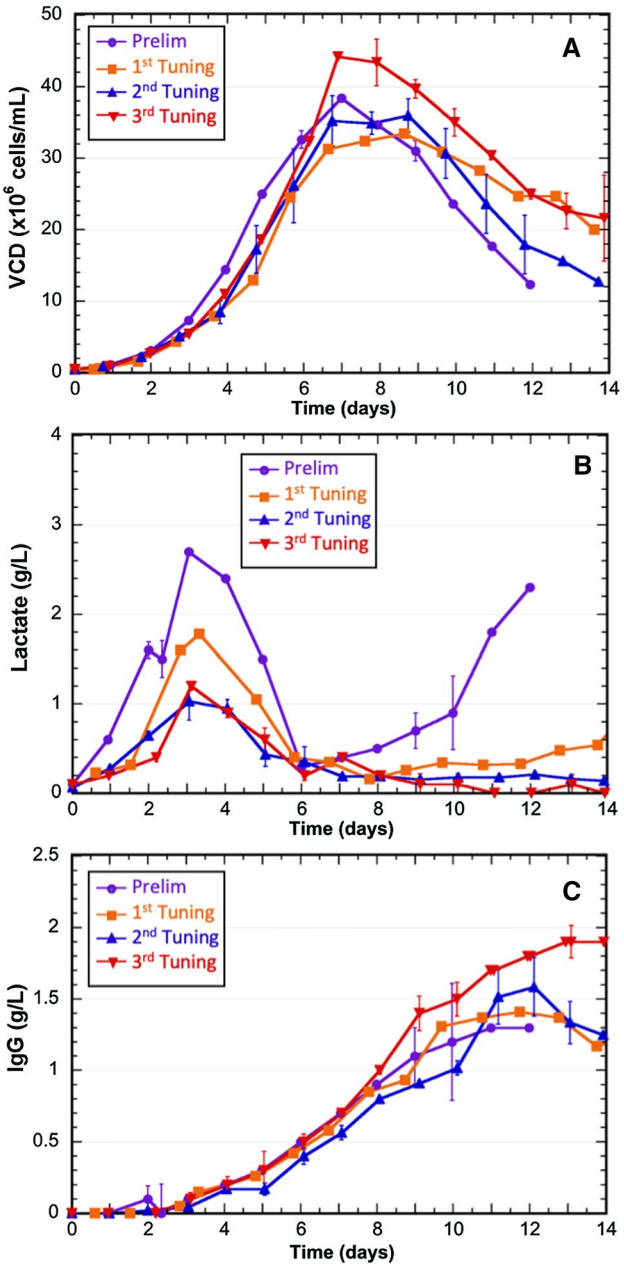

Fig. 4 Growth, lactate, and titers across the PID tuning experiments. Growth and metabolites profiles were obtained for the preliminary ambr250 experiment and the successive tuning experiments for CHO VRC01 cells using the same feed protocol. **A** Viable cell density (VCD). **B** Lactate; and **C** IgG (titer). Data are shown for the preliminary ambr250 bioreactors (purple), 1st tuning (orange), 2nd tuning (blue), and 3rd tuning (red) experiments

3.4.1 Preliminary DO PID tuning experiment

In the preliminary ambr250 experiment, the stir speed was not increased until the DO deviation reached control level 4. This control level configuration does not leverage the most powerful actuators of the volumetric oxygen mass transfer coefficient (k_La). Explicitly, Van't Riet developed an empirical relationship for k_La that is dependent on the superficial gas velocity (v_s; m min^{-1}), power (*P; W*), Volume (*V;* m^3), and empirical constants (***K, a,*** and **b**) [46] as shown in Eq. (1).

$$k_L a = K\left(\frac{P}{V}\right)^a v_S^b. \tag{1}$$

Since power is dependent on the stir speed (N, rpm) and impeller diameter (D_i; m) it can be calculated using Eq. (2),

$$P = N_P N^3 D_i^5, \tag{2}$$

where N_P (unitless) is an empirical correlation for different impeller type that is dependent on the Reynold's number, v_S is dependent on the gas flow rate (F; mL min^{-1}), and vessel cross-sectional area (A; m^2) as shown in Eq. (3) [47].

$$v_S = \frac{F}{A}. \tag{3}$$

Goldrick et al. obtained ***K, a,*** and ***b*** constants for an ambr15 and other common bioreactors, which ranged from 0.16 to 0.6 for ***a***, and 0.30 to 0.43 for ***b*** [47]. Interestingly, Van't Riet observed these constants to range $0.4 < \boldsymbol{a} < 1$ and $0 < \boldsymbol{b} < 0.70$ [46]. By substituting the power equation into the Van't Riet k_La equation, a nearly linear dependence on the stir speed and a lower power dependence on the gas flow rate becomes apparent. The DO represents the balance between and the oxygen uptake rate (OUR*)* by the cells and the oxygen transfer rate (OTR), given by Eq. (4):

$$\frac{d(DO)}{dt} = OTR - OUR, \tag{4}$$

where OUR is dependent on the VCD and cell specific oxygen uptake rate (q_{O_2}; mg O_2 $cell^{-1}$ h^{-1}) shown in Eq. (5):

$$OUR = q_{O_2}(VCD), \tag{5}$$

and the oxygen transfer rate (*OTR)* is defined in Eq. (6):

$$OTR = k_L a(C^* - DO), \tag{6}$$

where C^* is the oxygen saturation concentration of in the fluid (mg L^{-1}) and DO represents the oxygen concentration in the fluid (converted to mg L^{-1}). Thus, O_2 enrichment can increase the OTR fivefold when the DO approaches zero and fourfold when near setpoint, since C* is directly propotional to the O_2 partial pressure and Henry's constant, following Eq. (7).

$$\frac{d(DO)}{dt} = k_L a(C^* - DO) - q_{O_2}(VCD). \tag{7}$$

Therefore, the control levels were reorganized for the PID tuning experiments to leverage stir speed more effectively. Figure 3B shows the stir speed range changes in control level 2, alternating with O_2 enrichment.

3.4.2 First DO PID tuning experiment

For the DO PID tuning, it was desired to have multiple control levels to approximate simultaneous control using sequential control levels. The starting number of control levels for DO control in the first PID tuning experiment was 14 as shown in Fig. 3B. The manipulated variable ranges are graphically shown in Fig. 3B, and the PID gains for all 14 control levels are listed in Table 2. Initially, the DO response had oscillatory behavior, but on Day 2.6, an antifoam addition resulted in a slow and long DO recovery back to the setpoint (Fig. 2D). To address the long recovery, all t_I's were changed from 500 to 250 s on Day 4.7. The following day, it was determined tuning 14 control levels was too complex, as a single disturbance would pass through several control levels and confound tuning any one level. Therefore, the number of control levels was reduced to 10. Table 2 lists the revised PID gains and the manipulated variable ranges used in the first tuning experiment. As response times were still long, on Day 6.9, t_I was decreased from 250 to 100 s for all levels (Fig. 2D). Further, on Day 7.7, the control level 2 stir speed, k_P term was increased from 0.1 to 3.5 to match the k_P of the other stir speed gain values. Additionally, the t_D value was adjusted for control level 8 (O_2 enrichment) and control level 9 (O_2 flow rate) from 0 to 0.02 s. These adjustments decreased the noise in the DO response; however, the responses to the feed and antifoam additions became too slow. To address this, on Day 8.7, the t_D term was returned to 0 s. In order to observe the DO responses due to the differential term, on Day 10.7, the t_D term was increased from 0 to 0.02 s for multiple stir speed control level (control levels 2, 5, and 7), and O_2 enrichment control levels (control level 4). These adjustments resulted in noisy DO profiles; however, this was near the end of the process, so the VCD and productivity were not greatly affected (Fig. 4A, C).

3.4.3 Second DO PID tuning experiment

To further reduce the complexity of the DO PID tuning, the number of control levels was reduced for the second PID tuning experiment from 10 to 6 control levels. This reduction was guided by comparing the gas and stir profiles (Fig. 3F)

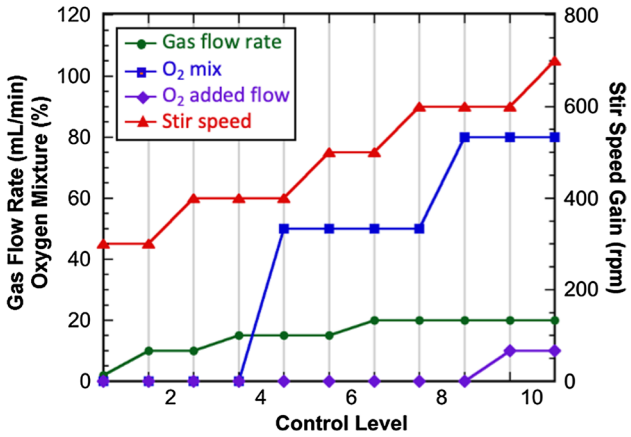

Fig. 5 Revised manipulated variable range profile. For the 1st tuning, the 14 control levels were replaced with 10 control levels on Day 5.6. The total gas flow rate to the sparge gas (Gas flow rate, green), an O_2 enrichment into the air/gas stream (O_2 mix, blue), O_2 flow rate added to the total gas flow rate (O_2 add flow, purple), and the stir speed (Stir speed, red)

with the revised first tuning experiment manipulated variable graph (Fig. 5). It was determined that control levels 9 and 10 were never used, while control level 6 was only briefly engaged. Specifically, between Days 6 and 9 and again around Day 12, control level 5 increased the stir speed from 400 to 500 rpm and then control level 7 quickly increase the stir speed to 600 rpm. These stir speed increases occurred without noticeable pause for the gas flow rate, which was controlled by control level 6. These observations warranted the reduction of control levels from 10 to 6 control levels. Table 2 lists the PID gains and manipulated variable ranges. Figure 3C shows the graphical representation of the manipulated variables for the second tuning experiment. These PID settings allowed for the process to have alternating O_2 enrichment and stir speed.

For the second DO PID tuning experiment, the DO profile oscillated through Day 2, yet DO was never lower than 40% (Fig. 2F), which was also observed in the pH profile (Fig. 2E). On Day 4, the first antifoam addition resulted in a more stable DO response compared to the first tuning experiment. However, as the VCD increased, the O_2 required by the cells increased, and in conjunction with an antifoam addition on Day 5, the DO profile decreased to 20%. On Day 6, the combination of the feed and antifoam additions allowed the DO to briefly go to zero. On Day 6.4, the t_D term was decreased from 0.02 to 0 for control levels 2 and 4 (O_2 enrichment). Recall due to Henry's Law and Eq. (7), O_2 enrichment has a strong effect on k_La and the rate of DO change, thus has the potential to cause overshooting if implemented faster than the system dyanmics. To reduce the disturbance magnitude, the antifoam addition volume was halved from 10 to 5 µL starting on Day 7.1. This stabilized DO, but antifoam additions were needed twice as often. On Day 9.2, the t_I term was decreased from 500 to 100 s for all control levels except control level 4 (O_2 enrichment) (Fig. 2F). This improved the DO response to the antifoam additions. On Day 10.2 for control level 4, the t_I term was decreased from 500 to 100 s. As the cultures are less active in this phase of the culture (in the decline phase for growth, Fig. 4A), it is unclear if these changes were the sole effect on the DO responses.

As there is no sufficiently detailed mammalian cell model that captures the interaction effects of pH and DO control, another approach was used. In this alternative approach, testing the PID settings at another site is considered acceptable. The initial PID setting from the second tuning experiment were transferred to the ambr250 located at the University of Delaware. While the second tuning experiments were being conducted in parallel, the University of Delaware ran two bioreactors using the Clemson PID settings. In the supplement, Fig S1, the outcomes are shown with the Clemson outcomes for VCD, lactate, and titer profiles. These data indicate the PID settings resulted in similar growth, lactate, and titer profiles.

3.4.4 Third DO PID tuning

The third tuning experiment was a validation experiment; however, a sudden drop in DO mid-experiment prompted some PID gain and manipulated variable adjustments. Based on the second tuning results, most of the PID gains matched the second tuning experiment except for control levels 2 and 4 (O_2 enrichment). The k_P term was increased three-fold (from 0.05 to 0.15 s) and t_D value was increased from 0 to 0.02 s, as O_2 enrichment has a pronounced impact on OTR based on Eq. (7). For control level 3, the stir speed k_P term was selected to be 2.0 instead of 3.5, while for control level 5, the k_P term was selected to be 1.0. These adjustments were implemented to allow slightly slower stir speed responses. Also, the k_P term for the added O_2 flow rate was increased from 0.1 to 0.5 to increase the output directly as this was the last control level for DO. Figure 3D graphically represents the manipulated variable ranges and Table 2 lists the PID gains. Despite

the new PID gains responsiveness, the DO profile on Day 7.8 deviated to low DO values overnight (Fig. 2H). When this was noticed (Day 8.4), the first response was to increase the maximum stir speed from 600 to 700 rpm, as the sparge gas was already 100% O_2 and the added O_2 had not been sufficient. Then, on Day 9.3, the maximum stir speed manipulated range was further increased from 700 to 850 rpm. Interestingly, the effect was more profound on the pH than on the DO.

Stir speeds above 600 rpm were not recommended by the NIH VRC researchers, so these high required stir speed were some concern. Yet, the VCD and titer were acceptable. In a review of the parameters reported to us by NIH, they indicated a 3-L Applikon vessel was used with a stir speed up to 200 rpm and a volume per volume gas flow rate of 0.14 vvm using air and O_2 sparging. The Applikon vessel had two 10 cm diameter marine impeller, where as the ambr250 has two 2.6 cm diameter marine impellers. Xu et al. compared the scale-down models of constant P/V and constant vvm with constant k_La for an ambr250 [10]. They observed that the ambr250 typically had lower k_La with similar vvm's compared to glass vessels. P. Xu et al. (2017) were concerned about shear in the ambr250. Further, Xu et al. conducted similar studies across production vessels [48]. Since the superficial gas velocities were similar between the ambr250 and glass vessels, the main effectors were the stir speed and impeller diameters. Based on constant P/V, stir speed for the ambr250 should have been 490 rpm to match 200 rpm in the Applikon [See Eqs. (1) and (2) for constant P/V dependencies or Xu et al.]. Interestingly, based on a constant shear between scales, the stir speed for the ambr250 could have gone up to 770 rpm, since this relationship is linear in stir speed and impeller diameter. Based on these calculations and the acceptable results on the third tuning experiment, future experiments will limit the stir speed to 770 rpm. This will potentially require high sparge gas flow rates to compensate.

It was encouraging that the VCD values for the third PID tuning experiment reached 45×10^6 cells mL^{-1} and the titers reached 2.0 g L^{-1}. These VCD and titers exceeded or matched the values from the traditional glass vessels, respectively (Fig. 4C). Yet, the cell specific productivity was still lower for the ambr250 runs compared to the traditional glass vessels. Analysis of the glycan profiles and other metabolites, including amino acids, could provide information about how to increase the cell specific titers such that the ambr250 and glass vessels have similar cell specific productivities as well. However, within the CHOg2p studies, the current PID gains and manipulated ranges profile a robust culture environment.

The robustness of the third PID tuning settings was investigated by using these settings across two CHO cell lines and three media and feeding schemes. In the supplement, Fig S2, shows the outcomes for VCD, lactate, and titer profiles for these four diffident combinations. This data indicate the PID settings resulted in similar growth, lactate, and titer profiles. In Fig S3, the pH and DO profiles are shown, and demonstrate that DO was very well controlled to the setpoint, which were 50% DO for the CHO VRC01 cell line and 30% DO for the CHOZN GS23 (Millipore Sigma). For pH, the manipulated variables were the same as developed by the third PID tuning experiment, except the setpoints were varied to examine the effect of pH on outcomes, specifically the productivity (titer). Therefore, in Fig S3, note the pH has several setpoints and additionally, DBs were used. In all cases, the pH was stablily controlled. In most cases, the pH was observed to be at the upper DB, as the CO_2 flowrate was limited to avoid high pCO_2. As these and similar cultures have been observed to have elevated pCO_2 values, future work will focus on methods to decrease the pCO_2.

Further, comparisons of the DO profiles across the preliminary and PID tuning experiments demonstrates that the tuning improved the DO control (Fig. 2B, D, F, H). The root of this success was the decreased lactate accumulation mid-culture (Fig. 4B). Future work will examine the off-gas profiles and alternative base control solutions, such as sodium carbonate vs the sodium bicarbonate that was used in these studies. Additionally, accurate process models for mammalian cell culture would aid PID tuning, as has been observed for microbial cultures [19], yet would also need to account for interactions between the bicarbonate buffer and cell metabolism [22, 37].

4 Conclusions

In summary, trial and error PID tuning is still required for the ambr®250 bioreactor system, as the sequential control levels increase the complexity to refine these PID gains and manipulated variable ranges. Further, no process model exists that incorporates accurately the interactions between the bicarbonate buffer and cell metabolism. Unlike traditional chemical processes, the PID gains cannot be set to zero and gradually increased. Great care must be taken to avoid confounding the PID tuning for biological processes to avoid cell death, especially for mammalian cell cultures. As mammalian cell culture biological processes are highly dynamic and more sensitive to disturbances, it is best to wait for natural process disturbances to occur to minimize negative outcomes while PID tuning. Since the PID gains and manipulated variable ranges can affect the process outcomes, even with similar feeding protocols and a single cell line, PID gains and

manipulated variable ranges should be routinely specified in publications. If PID gains and manipulated variable ranges are not specified, it may not be possible to reproduce the experimental results.

Acknowledgements This work was funded by the National Science Foundation Grants IIP-1624641, OIA-1736123 and Advanced Mammalian Biomanufacturing Innovation Center (AMBIC) award 2016-01. As ambr250 requires a team to run, we would like to acknowledge experimental assistance from Shanice Flournoy, Benjamin F. Synoground, Claudia Sisk, Lisa Uy, and Dylan Chitwood. We also wish to acknowledge Dylan Chitwood for careful review of the manuscript.

Research Resource Identifiers (RRID) Cell Line: Chinese hamster ovary (CHO) cell line RRID: CVCL_0213. Antibody: HIV Envelope CD4 binding site RRID: AB_2491019.

Authors' contributions KSE, SRK, and HD conducted the experiments, while SWH and BAS participated in the PID tuning part of the experiments. SWH wrote the main manuscript text and prepared the graphics. KSE and BAS reviewed and edited the manuscript critically for important intellectual content. KHL reviewed the manuscript and provided critical comments. All authors read and approved the final manuscript.

Funding This work was funded by the National Science Foundation Grants IIP-1624641, OIA-1736123 and Advanced Mammalian Biomanufacturing Innovation Center (AMBIC) award 2016-01.

Data availability The datasets generated during and/or analysed during the current study are available from the corresponding author on reasonable request.

Declarations

Competing interests The authors declare no financial or commercial competing interests.

References

1. Freund NW, Croughan MS. A simple method to reduce both lactic acid and ammonium production in industrial animal cell culture. Int J Mol Sci. 2018;19(2):385. https://doi.org/10.3390/ijms19020385.
2. Ryll T, Valley U, Wagner R. Biochemistry of growth inhibition by ammonium ions in mammalian cells. Biotechnol Bioeng. 1994;44(2):184–93. https://doi.org/10.1002/bit.260440207.
3. Lao MS, Toth D, Danell G, Schalla C. Degradative activities in a recombinant Chinese hamster ovary cell culture. Cytotechnology. 1997;24(3):263.
4. Genzel Y, Ritter JB, Konig S, Alt R, Reichl U. Substitution of glutamine by pyruvate to reduce ammonia formation and growth inhibition of mammalian cells. Biotechnol Prog. 2005;21(1):58–69. https://doi.org/10.1021/bp049827d.
5. Yang M, Butler M. Effects of ammonia and glucosamine on the heterogeneity of erythropoietin glycoforms. Biotechnol Prog. 2002;18(1):129–38. https://doi.org/10.1021/bp000090b.
6. Xu S, Gavin J, Jiang RB, Chen H. Bioreactor productivity and media cost comparison for different intensified cell culture processes. Biotechnol Prog. 2017;33(4):867–78. https://doi.org/10.1002/btpr.2415.
7. Fan Y, Jimenez Del Val I, Müller C, Wagtberg Sen J, Rasmussen SK, Kontoravdi C, et al. Amino acid and glucose metabolism in fed-batch CHO cell culture affects antibody production and glycosylation. Biotechnol Bioeng. 2015;112(3):521–35. https://doi.org/10.1002/bit.25450.
8. Handlogten MW, Wang J, Ahuja S. Online control of cell culture redox potential prevents antibody interchain disulfide bond reduction. Biotechnol Bioeng. 2020;117(5):1329–36. https://doi.org/10.1002/bit.27281.
9. Hoshan L, Jiang RB, Moroney J, Bui A, Zhang XL, Hang TC, et al. Effective bioreactor pH control using only sparging gases. Biotechnol Prog. 2019;35(1):e2743. https://doi.org/10.1002/btpr.2743.
10. Xu P, Clark C, Ryder T, Sparks C, Zhou J, Wang M, et al. Characterization of TAP Ambr 250 disposable bioreactors, as a reliable scale-down model for biologics process development. Biotechnol Prog. 2017;33(2):478–89. https://doi.org/10.1002/btpr.2417.
11. Xu S, Hoshan L, Chen H. Improving lactate metabolism in an intensified CHO culture process: productivity and product quality considerations. Bioprocess Biosyst Eng. 2016;39(11):1689–702. https://doi.org/10.1007/s00449-016-1644-3.
12. Tai M, Ly A, Leung I, Nayar G. Efficient high-throughput biological process characterization: definitive screening design with the Ambr250 bioreactor system. Biotechnol Prog. 2015;31(5):1388–95. https://doi.org/10.1002/btpr.2142.
13. Yee JC, Rehmann MS, Yao G, Sowa SW, Aron KL, Tian J, et al. Advances in process control strategies for mammalian fed-batch cultures. Curr Opin Chem Eng. 2018;22:34–41. https://doi.org/10.1016/j.coche.2018.09.002.
14. Madhuranthakam CR, Elkamel A, Budman H. Optimal tuning of PID controllers for FOPTD, SOPTD and SOPTD with lead processes. Chem Eng Process Process Intensif. 2008;47(2):251–64. https://doi.org/10.1016/j.cep.2006.11.013.
15. Ziegler JG, Nichols NB. Optimum settings for automatic controllers. Trans ASME. 1942;64:759–68.
16. Cohen GH, Coon GA. Theoretical consideration of retarded control. Trans ASME. 1953;75:827–34.
17. Smith CL, editor. Practical process control: tuning and troubleshooting 2009.

18. Rathore AS, Mishra S, Nikita S, Priyanka P. Bioprocess control: current progress and future perspectives. Life Basel. 2021;11(6):557. https://doi.org/10.3390/life11060557.
19. Khan O, Madhuranthakam CMR, Douglas P, Lau H, Sun J, Farrell P. Optimized PID controller for an industrial biological fermentation Cheek for process. J Process Control. 2018;71:75–89. https://doi.org/10.1016/j.jprocont.2018.09.007.
20. MarsiliLibelli S, Beni S. Shock load modelling in the anaerobic digestion process. Ecol Model. 1996;84(1–3):215–32. https://doi.org/10.1016/0304-3800(94)00125-1.
21. Doi T, Kajihara H, Chuman Y, Kuwae S, Kaminagayoshi T, Omasa T. Development of a scale-up strategy for Chinese hamster ovary cell culture processes using the k(L)a ratio as a direct indicator of gas stripping conditions. Biotechnol Prog. 2020. https://doi.org/10.1002/btpr.3000.
22. Goudar CT, Piret JM, Konstantinov KB. Estimating cell specific oxygen uptake and carbon dioxide production rates for mammalian cells in perfusion culture. Biotechnol Prog. 2011;27(5):1347–57. https://doi.org/10.1002/btpr.646.
23. Lu F, Toh PC, Burnett I, Li F, Hudson T, Amanullah A, et al. Automated dynamic fed-batch process and media optimization for high productivity cell culture process development. Biotechnol Bioeng. 2013;110(1):191–205. https://doi.org/10.1002/bit.24602.
24. Wlaschin KF, Hu WS. Fedbatch culture and dynamic nutrient feeding. In: Hu WS, Scheper T, editors. Cell Culture Engineering. Advances in Biochemical Engineering-Biotechnology, 2006. p. 43–74.
25. Simon L, Karim MN. Identification and control of dissolved oxygen in hybridoma cell culture in a shear sensitive environment. Biotechnol Prog. 2001;17(4):634–42. https://doi.org/10.1021/bp010044r.
26. Leva A, Papadopoulos AV. Teaching a conscious use of PI/PID tuning rules. IFAC Proc Vol. 2013;46(17):25–30. https://doi.org/10.3182/20130828-3-UK-2039.00007.
27. Chotteau V, Hjalmarsson H, editors. Tuning of dissolved oxygen and pH PID control parameters in large scale bioreactor by lag control. In: 21st Annual Meeting of the European-Society-for-Animal-Cell-Technology (ESACT); 2009 Jun 07–10; Dublin, IRELAND2012.
28. Martens DE, van den End EJ, Streefland M. Configuration of Bioreactors. In: Portner R, editor. Animal Cell Biotechnology: Methods and Protocols, 3rd Edn. Methods in molecular biology, 2014. p. 285–311.
29. Rameez S, Mostafa SS, Miller C, Shukla AA. High-throughput miniaturized bioreactors for cell culture process development: reproducibility, scalability, and control. Biotechnol Prog. 2014;30(3):718–27. https://doi.org/10.1002/btpr.1874.
30. Longsworth J, Schillings N, Sha M. Dissolved oxygen control PID tuning for cell culture applications. In: Eppendorf, editor. Eppendorf Enfield, CT, USA: Eppendorf Bioprocess Center; 2020.
31. Elliott K, Harris G, Harcum S, Blakeman K, Gavin C, Anderson J. Spent media analysis with an integrated CE-MS analyzer of chinese hamster ovary cells grown in an ammonia-stressed parallel microbioreactor platform. BioProcess J. 2020;19. https://doi.org/10.12665/J19OA.ElliottJournal.
32. Synoground BF, McGraw CE, Elliott KS, Leuze C, Roth JR, Harcum SW, et al. Transient ammonia stress on Chinese hamster ovary (CHO) cells yield alterations to alanine metabolism and IgG glycosylation profiles. Biotechnol J. 2021;16(7):2100098. https://doi.org/10.1002/biot.202100098.
33. Chitwood DG, Wang Q, Elliott K, Bullock A, Jordana D, Li Z, et al. Characterization of metabolic responses, genetic variations, and microsatellite instability in ammonia-stressed CHO cells grown in fed-batch cultures. BMC Biotechnol. 2021;21(1):4. https://doi.org/10.1186/s12896-020-00667-2.
34. Seifter JL, Chang HY. Extracellular acid–base balance and ion transport between body fluid compartments. Physiology. 2017;32(5):367–79. https://doi.org/10.1152/physiol.00007.2017.
35. Pepper ME, Wang L, Padmakumar A, Burg TC, Harcum SW, Groff RE et al. A CMI (cell metabolic indicator)-based controller for achieving high growth rate *Escherichia coli* Cultures. In: 2014 36th Annual International Conference of the IEEE Engineering in Medicine and Biology Society. IEEE Engineering in Medicine and Biology Society Conference Proceedings, 2014. p. 2911–5.
36. Xu B, Jahic M, Blomsten G, Enfors SO. Glucose overflow metabolism and mixed-acid fermentation in aerobic large-scale fed-batch processes with *Escherichia coli*. Appl Microbiol Biotechnol. 1999;51(5):564–71.
37. Goudar CT, Matanguihan R, Long E, Cruz C, Zhang C, Piret JM, et al. Decreased pCO_2 accumulation by eliminating bicarbonate addition to high cell-density cultures. Biotechnol Bioeng. 2007;96(6):1107–17. https://doi.org/10.1002/bit.21116.
38. Mulukutla BC, Gramer M, Hu WS. On metabolic shift to lactate consumption in fed-batch culture of mammalian cells. Metab Eng. 2012;14(2):138–49. https://doi.org/10.1016/j.ymben.2011.12.006.
39. Kimura R, Miller WM. Effects of elevated pCO_2 and/or osmolality on the growth and recombinant tPA production of CHO cells. Biotechnol Bioeng. 1996;52:152–60.
40. deZengotita VM, Schmelzer AE, Miller WM. Characterization of hybridoma cell responses to elevated pCO_2 and osmolality: Intracellular pH, cell size, apoptosis, and metabolism. Biotechnol Bioeng. 2002;77(4):369–80.
41. O'Brien CM, Zhang Q, Daoutidis P, Hu W-S. A hybrid mechanistic-empirical model for in silico mammalian cell bioprocess simulation. Metab Eng. 2021;66:31–40. https://doi.org/10.1016/j.ymben.2021.03.016.
42. Xing ZZ, Lewis AM, Borys MC, Li ZJ. A carbon dioxide stripping model for mammalian cell culture in manufacturing scale bioreactors. Biotechnol Bioeng. 2017;114(6):1184–94. https://doi.org/10.1002/bit.26232.
43. Chopda V, Gyorgypal A, Yang O, Singh R, Ramachandran R, Zhang H, et al. Recent advances in integrated process analytical techniques, modeling, and control strategies to enable continuous biomanufacturing of monoclonal antibodies. J Chem Technol Biotechnol. 2021. https://doi.org/10.1002/jctb.6765.
44. Wasalathanthri DP, Rehmann MS, Song Y, Gu Y, Mi L, Shao C, et al. Technology outlook for real-time quality attribute and process parameter monitoring in biopharmaceutical development—a review. Biotechnol Bioeng. 2020;117(10):3182–98. https://doi.org/10.1002/bit.27461.
45. Mulukutla BC, Yongky A, Grimm S, Daoutidis P, Hu WS. Multiplicity of steady states in glycolysis and shift of metabolic state in cultured mammalian cells. PLoS ONE. 2015;10(3):e0121561. https://doi.org/10.1371/journal.pone.0121561.
46. Van't RK. Review of measuring methods and results in nonviscous gas-liquid mass-transfer in stirred vessels. Ind Eng Chem Process Des Dev. 1979;18(3):357–64. https://doi.org/10.1021/i260071a001.
47. Goldrick S, Lee K, Spencer C, Holmes W, Kuiper M, Turner R, et al. On-line control of glucose concentration in high-yielding mammalian cell cultures enabled through oxygen transfer rate measurements. Biotechnol J. 2018;13(4):1700607. https://doi.org/10.1002/biot.201700607.

48. Xu S, Hoshan L, Jiang RB, Gupta B, Brodean E, O'Neill K, et al. A practical approach in bioreactor scale-up and process transfer using a combination of constant P/V and vvm as the criterion. Biotechnol Prog. 2017;33(4):1146–59. https://doi.org/10.1002/btpr.2489.